Blind Modulation Classification for Cognitive Satellite in the Spectral Coexistence Context

Vincent Gouldieff, Jacques Palicot, Steredenn Daumont

▶ **To cite this version:**

Vincent Gouldieff, Jacques Palicot, Steredenn Daumont. Blind Modulation Classification for Cognitive Satellite in the Spectral Coexistence Context. IEEE Transactions on Signal Processing, 2017, 65 (12), pp.3204-3217. 10.1109/TSP.2017.2688976 . hal-01513362

HAL Id: hal-01513362
https://hal.science/hal-01513362

Submitted on 25 Apr 2017

HAL is a multi-disciplinary open access archive for the deposit and dissemination of scientific research documents, whether they are published or not. The documents may come from teaching and research institutions in France or abroad, or from public or private research centers.

L'archive ouverte pluridisciplinaire **HAL**, est destinée au dépôt et à la diffusion de documents scientifiques de niveau recherche, publiés ou non, émanant des établissements d'enseignement et de recherche français ou étrangers, des laboratoires publics ou privés.

Blind Modulation Classification for Cognitive Satellite in the Spectral Coexistence context

Vincent Gouldieff, *Member, IEEE,* Jacques Palicot, *Member, IEEE,* and Steredenn Daumont, *Member, IEEE*

***Abstract*—The scarcity of the usable satellite spectrum has led to a need for advanced communication techniques. Among them, multi-satellite networks have been promoted for their ability to reuse the frequency bands in a more aggressive manner. This is made possible by sharing both the spectral and spatial degrees of freedom. Meanwhile, the concept of Cognitive Satellite (CS) was deeply investigated to make the best of these novel architectures. In this context, very few blind signal processing methods were proposed to tackle the co-channel interference issues entailed by such systems. Herein, we develop a novel low-complexity algorithm for blind Automatic Modulation Classification (AMC) and parameters estimation in the strongly interfering scenario. The proposed method rely on an Analytical study of the Mth-Power nonlinear Transformation (AMPT) of the co-channel mixture. Theoretical analysis and extensive simulations show the effectiveness of the proposed method in various scenarios.**

***Index Terms*—Blind Signal Processing, Cognitive Satellite, Coexistence Scenario, Automatic Modulation Classification, M^{th}-Power nonlinear Transformation.**

I. Introduction

NEXT generation of Satellite Communications (SatComs) systems mainly aims at enhancing the global network throughput while ensuring Quality of Service (QoS) [1]. The advent of multi-satellite and hybrid networks using multibeam technologies has led to numerous spectrum sharing techniques [2]. To push the global capacity optimization into a corner, the concept of Cognitive Radio [3] has been considered for SatComs to make the best use of the available diversities (e.g., spectral, temporal, spatial diversities). The paradigm of Cognitive Satellite [4] was born. Thereby, strong co-channel interference may occur between the primary link and the secondary links at both the uplink and the downlink. For instance, such a scenario is encountered when two or more multibeam satellites share the same geographic region [5] or when a cellular network is built on a dual-satellite system [6].

In the cognitive context, several features of the interfering signals may be dynamically chosen so that the spectral efficiency is maximized [7]. In order to cut the overhead down, these parameters are not transmitted and it becomes mandatory to estimate them at the receiver [8]. Classical methods of blind signal processing applied on the entailed co-channel mixture rapidly show their limits. Their inability to correctly infer the Signal-of-Interest (SoI) is all the more true when the composite power of the interferers grows. Actually, while the SINR (Signal to Interference-plus-Noise Ratio) of the SoI weakens, the available statistical properties of the interferers are not exploited as useful information for the inference of the unknown features of the co-channel signals.

Consequently, classical[1] methods for Automatic Modulation Classification (AMC) applied on co-channel mixtures of signals perform poorly. This fact has recently motivated the scientific community to investigate the Multiuser[2] AMC (MAMC) issue. In the blind scenario, MAMC has long been seen as a real challenge which may explain why the Multiuser case is so sparse in the AMC literature (cf. Section III).

Thereby, very few MAMC methods were proposed, whether it was considered in the single-node or in the distributed multi-node contexts[3]. The latter would be preferred in interconnected networks provided for the purpose and in the military domain, where the data exchange between the nodes is not an issue. However, in the context of CR, the savings in terms of overhead would be mitigated by the consequent signaling between the nodes, needed to fusion the collected information. This fact has motivated the study of MAMC techniques in the terrestrial cognitive single-node context. To the best of our knowledge, Spooner was the first to propose an algorithm for MAMC in the single-node scenario, in 1996 [10]. Since then, it seems that no efficient and practically feasible algorithm has been proposed in the literature to face the blind single-node MAMC issue, which is precisely our goal.

Throughout this article, we actually are interested in the blind MAMC of asynchronously mixed co-channel signals received by a single antenna. More precisely, we are prone to consider the (almost-)totally spectral overlapping scenario. This case study is of real interest for three main reasons. First, the (almost-)totally overlapping scenario would appear in the context of Cognitive Satellite where time and frequency are slotted for an easier management of the resource. Secondly, the asynchronous assumptions can not be relaxed since perfect time/frequency alignment between the overlapping signals is generally not reachable. Finally, the considered scenario is a major issue in the field of MAMC: it actually seems that no proposed signal processing method is currently able to face it.

V. Gouldieff and J. Palicot are with the Signal, Communication and Embedded Electronics (SCEE) Research Team, CentraleSupelec/IETR, Avenue de la Boulaie - CS 47601, 35573 Cesson-Sevigne Cedex, France.
E-mail : vincent.gouldieff@supelec.fr, jacques.palicot@supelec.fr.

V. Gouldieff and S. Daumont are with Zodiac Data Systems SAS, 5 Esplanade Anton Phillips, 14460 Colombelles, France. Formerly, she was with the SCEE Research Team. E-mail : steredenn.daumont@zodiacaerospace.com.

[1]By "classical", we include all the AMC methods that are designed for a single signal corrupted by noise. Thereby, it is assumed that no interferer is spectrally overlapping with this signal whatsoever.

[2]The terminology "Multiuser AMC" (MAMC) was first proposed in 2012 by Zaerin et al., in [9]. MAMC refers to the AMC methods that are designed to face partial or total spectral overlapping of two or more signals.

[3]"Single-node" and "multi-node" refer to the number of terrestrial stations that are assumed to receive and process the mixture. In the satellite context, a "node" is composed of a single antenna since no spatial diversity is available.

The MAMC algorithm we propose in this article relies on an Analytical study of the M^{th}-Power Nonlinear Transformation (AMPT) [11]. As further discussed, this transform is chosen for its ability to blindly recognize the constellations of the co-channel signals at a small computational expense and with a good robustness against the unknown parameters. The whole method is classically structured around a two step architecture compounded of a preprocessing unit and a recognition algorithm, as depicted in Fig. 1.

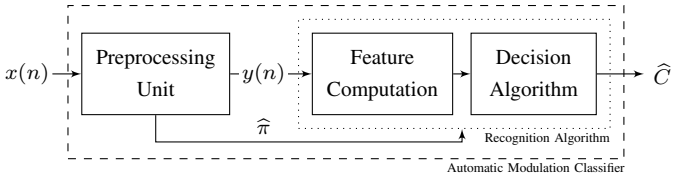

Fig. 1. The common Feature-Based AMC architecture

The paper is organized as follows: In Section II, we describe the considered scenarios and formulate the working hypothesis. In Section III a brief review of (M)AMC methods is unfolded, while in Sections IV to VII, we develop the underlying theory of AMPT for AMC and MAMC. In Section VIII, the proposed AMPT-based algorithms in the co-channel context are detailed. Finally, the performance of the proposed methods is studied via extensive simulations throughout Section IX.

II. Problem Statement

Thereby, we describe the scenarios entailing asynchronous co-channel interference of satellite signals, and we illustrate them with specific case-studies. Then, we derive the associated mathematical model and assumptions in the blind context.

A. System model and interference scenarios

Small satellite dishes (such as the one used in VSATs) are increasingly considered at the end users for their cost and space requirement. Due to their non-directivity, they willingly allow multi-satellite communications, but they also inherently induce unwanted interference at both the forward and the reverse links [12]. Thereby, we consider Geostationary (GEO) bent-pipe satellites used for Fixed Satellite Services (FSS).

1) Scenario A – Interference at the end user (Forward link): We may consider the scenario induced by the transmission of multiple gateways through closely located satellites. Interference occurs when their footprints and frequency plan overlap at the downlink (Fig. 2). It equivalently happens with a multibeam satellite when the frequency reuse policy is aggressive [13].

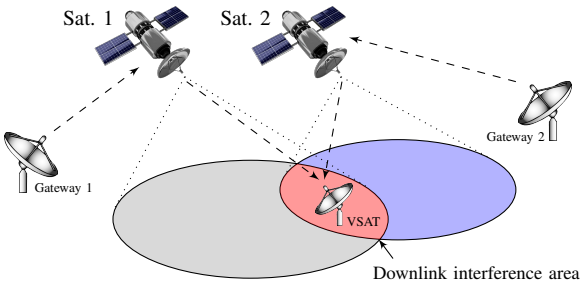

Fig. 2. Forward link interference at the VSAT due to overlapping footprints

2) Scenario B – Interference at one or more satellites from multiple VSATs (Reverse link): In the Cognitive Satellite context, multiple VSATs may jointly communicate with a primary and a secondary satellites. When these VSATs are all located in the same footprint, they may interfere at the uplink as shown in Fig. 3.

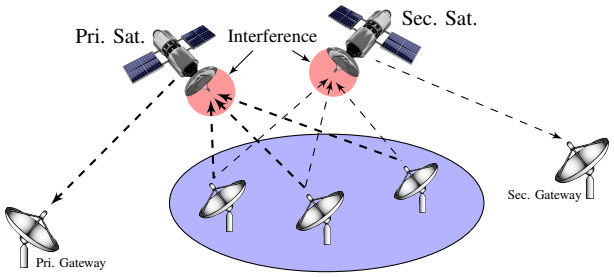

Fig. 3. Reverse link interference at the satellites from multiple VSATs

3) Case-studies for Scenarios A and B in the literature: Scenario A captures the case of coexistent multibeam GEO satellites in Ka band, as shown in [5] and [6]. In these articles, it is proposed to mitigate co-channel interference via coordination between the gateways. This assumption is in practice very restrictive and then we relax it in the present work.

Scenario B accurately models the interference produced by cognitive SatComs at the reverse link, as shown in scenarios D and E of the CoRaSat approach [14]. Thereby, some portions of the C and Ku bands are used on a primary basis by FSS. Non-directive terminals may produce significant interference due to their opportunistic link with a secondary satellite.

B. Mathematical model of the involved co-channel mixture

We derive the expression of the mixture at the VSAT for the forward link (Scenario A). The derivation for Scenario B is similar and leads to an analogous model with the same mathematical structure. First, the uplink signal at gateway u is expressed in baseband as

$$x_u(t) = \sum_{k\in\mathbb{Z}} s_u(k)\cdot h_u(t-kT_u), \tag{1}$$

where s_u is the $i.i.d.$ symbol stream carried by constellation $C_u \in \mathcal{C}$, h_u the pulse-shaping function and T_u the symbol time.

The physical link between each gateway u and the VSAT receiver (including the uplink, the bent-pipe satellite and the downlink) is classically modeled for fixed satellite systems as a delayed single-path channel $h_u^p(t)$ such that

$$h_u^p(t) = a_u \cdot e^{i(2\pi f_u t+\phi_u)}\cdot\delta(t-\tau_u), \tag{2}$$

where a_u is the amplitude, f_u the carrier frequency at the downlink, ϕ_u the initial phase and τ_u the delay. You may refer to Section II.C for the detailed assumptions related to the aforementioned parameters.

Denoting $\mathbf{x}(t) = [x_1, \cdots, x_U]$ and $\mathbf{h_u^p}(t) = [h_1^p, \cdots, h_U^p]^T$ with U the number of signals sharing the same band, we get at the receiver the following co-channel mixture of signals:

$$x(t) = \mathbf{x}(t)\cdot\mathbf{h_u^p}(t) + \nu(t), \tag{3}$$

where $\nu(t)$ stands for Additive White Gaussian Noise (AWGN) with unknown variance σ_ν^2.

At the receiver, signal $x(t)$ is sampled (to output $x(n)$) and blindly preprocessed (to output $y(n)$), as described in Fig. 1. The latter task includes a translation to pseudo base-band – i.e. the resultant Power Spectral Density (PSD) is located at a frequency f_{ry} which is close to zero – and a normalization step – as the one proposed in [11] – so that the noise-free mixture has unit power. A low-pass pre-filter is also considered for a better rejection of adjacent channels and out-of-band noise.

The discrete time samples $y(n)$ obtained at the output of the preprocessing unit are then equivalently given by

$$y(n) = \sum_{u=1}^{U} y_u(n) + \nu(n), \tag{4}$$

where, $y_u(n)$ corresponds to the u^{th} signal component:

$$y_u(n) = a_u \cdot e^{i(2\pi f_{ru} n + \phi_u)} \sum_{k \in \mathbb{Z}} s_u(k) h_u\left(nT_e - kT_u - \tau_u\right), \tag{5}$$

where T_e denotes the sampling period and f_{ru} the residual Carrier Frequency Offset (CFO) for signal u. Thereby, we classically consider that h_u are Root Raised Cosine (RRC) filters with unknown Roll-Off factor β_u.

C. Assumptions on the parameters in the realistic context

The satellite channels, in addition to the absence of synchronization at the gateways and satellites, inherently produce impairments between the downlink signals at the receiver.

1) Effects induced by the Local Oscillators (LO): The LO have an impact on carrier frequency and symbol time. In fact, denoting ϵ_u the summed LO imprecisions of link u, the received carrier frequency at the VSAT is $f_u = (1+\epsilon_u) \cdot f_c$, with f_c the target downlink carrier frequency. In the same way, we have $T_u = (1+\epsilon_u) \cdot T$, with T the target symbol rhythm.

Considering a standard value of around 0.1 ppm for ϵ_u [15], a bandwidth B of the order of the MHz and the use of C, Ku or Ka band lead to the following mathematical properties:

- For all u, T_u is considered to all be almost equal T.
- For all u, the CFO f_{ru} is small compared to T such that the "almost-overlapping" scenario holds. Without loss of generality (wlog), we assume in this work that the f_{ru} are all different, even slightly, with probability one.

A graphical representation of these effects is shown in Fig. 4 for a mixture of 3 signals. The CFOs have been voluntarily overstated for a better readability. The dashed line represent the shape of the low-pass pre-filter in the preprocessing unit. Last, P_u stands for the power of signal u and P_y for the summed power in band B, so that $P_y - P_\nu = 1$.

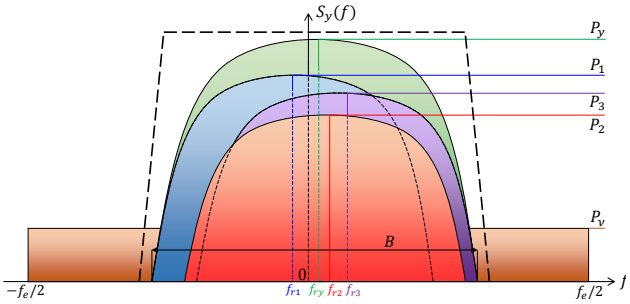

Fig. 4. Representation of the PSDs of the co-channel signals

At the receiver, we assume that a proper algorithm, such as the one in [16], estimates T. The residual CFOs are assumed as unknown: they are estimated by the proposed MPT method.

2) Other assumptions on signal y_u: In (5), we assume that ϕ_u and τ_u are uniformly distributed, respectively in $[0; 2\pi[$ and $[0; T[$, and unknown. Note that unlike several AMC methods, we do not assume that $T_e = T$ (i.e. we do not perform any time synchronization at the receiver, which would be impractical in the interfering context). Instead, we assume that $y(n)$ is properly oversampled by a factor $\rho = T/T_e$ which respects Shannon's sampling theorem, i.e. $T_e^{-1} \geq B$.

3) Assumptions related to s_u and $\mathcal{C}$: Symbol sets s_u are independent and identically distributed, and respectively carried by constellations $C_u \in \mathcal{C}$. The C_u may all be different. All the C_u are zero mean, unit variance and unknown. Set $\mathcal{C}$, however, is assumed to be known. As depicted in Fig. 5, we consider PSK, QAM and "hybrid" constellations for the sake of a sufficient diversity. Moreover, these constellations are typically used in SatComs (see e.g., *IESS-310* and *ETSI EN 301 210*).

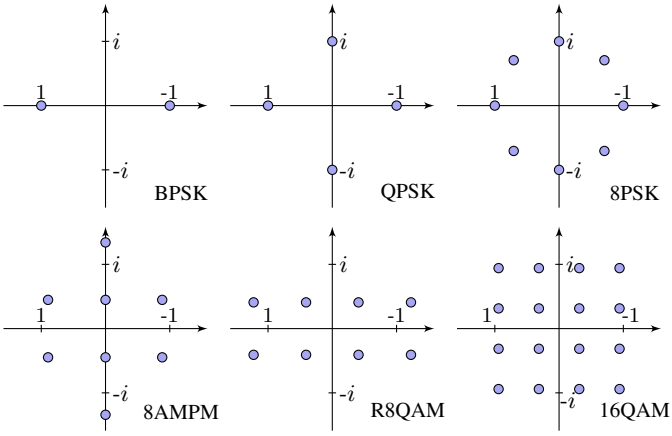

Fig. 5. Representation of the considered constellations in the complex plan

D. Overview of the assumptions

Table I sums up the assumptions proposed in the current Section as well as the blind aspects of the proposed method. Note that "Estimated with AMPT" means that we propose in this article an algorithm to blindly estimate the considered parameter. "$*$" means that no particular assumption is taken.

TABLE I
ASSUMPTIONS AND BLINDNESS OF THE PROPOSED METHOD

Para.	Assumption	Blind aspects
U	$U \geq 0$	Unknown, estimated with AMPT
T_u	$T_u \approx T$	Unknown, estimated with [16]
τ_u	$*$	Unknown
f_{ru}	$f_{ru} \neq$ pairwise, $\ll T^{-1}$	Unknown, estimated with AMPT
ϕ_u	$*$	Unknown
s_u	$i.i.d.$ symbol sets	Unknown
C_u	$C_u \in \mathcal{C}$	$\mathcal{C}$ is assumed to be known
a_u	$*$	Unknown, estimated with AMPT
h_u	pulse-shaping function	Known (down to the roll-off factor)
ν	AWGN	Unknown σ_ν^2, estimated with [11]
y	Norm. and oversampled	Blind normalization as in [11]

III. AMC AND MAMC: A PRACTICAL REVIEW

In this Section, we unfold a brief review of the general methods used in the literature for AMC and MAMC.

A. A brief review of AMC methods in the single-signal case

For the sake of a better understanding, it seems crucial to quickly draw a hierarchical inventory of classically used AMC algorithms in the single-signal case before outlining the formerly proposed MAMC methods.

Classically, the first step is to demodulate – e.g., normalize, filter and synchronize in time and/or frequency – the received signal. Then, a Likelihood-Based (LB) or a Feature-Based (FB) recognizer performs the constellation classification [17]. While LB algorithms are optimal in the likelihood sense – they use exact or approximated Likelihood Ratio Tests (LRT) as a decision criterion – FB methods are generally preferred for their robustness to model mismatch and their close-to-optimal performance at a lower computational complexity [18].

In the blind scenario, the performance of the whole AMC method relies on both the quality of the preprocessing step – which may be intricate in the blind context – and on the ability of the features to discriminate the constellations of a given set (Fig. 1). Several features have been proposed in the literature to classify both analog and digital modulations [18], such as Higher-Order Moments (HOM) and Higher-Order Cumulants (HOC) [19]. However, these features are very sensitive to time and frequency synchronizations: in the blind scenario, any estimation inaccuracy would lead to a substantial loss in the performance of the whole classifier. Mainly to improve the robustness against the unknown in the blind scenario, Cyclic Moments (CM), Cyclic Cumulants (CC) [20] and spectral non-linearities of the signal [11] were exploited as strong features for the blind classification of digital modulations.

B. Proposed MAMC methods in the co-channel context

Some of the features listed in Subsection III.A were also studied in the context of spectral overlapping communication signals in the single-node context (i.e. with a single antenna).

Spooner proposed a Minimum Distance (MD) classifier based on Cyclic Cumulants [10] [21] [22] as a solution to the MAMC issue. Thereby, the features used for the classification are chosen by puncturing the two-dimensional n^{th}-order Cyclic Temporal Cumulant Function (CTCF) at some specific frequencies and cyclic-frequencies for different values of n. The method aims at being blind and only requires the knowledge of a few parameters. It mostly uses the signal bandwidth and the pulse-shaping filter characteristics as discriminants: thus, it may not be directly applicable in the present case study.

Zaerin et al. proposed a second approach to tackle the single-antenna MAMC issue [9]. It relies on a MD classification based on some ratios of classical Higher Order Cumulants (HOCs). While this approach shows a very low complexity, its performance would quickly degrade in the blind scenario with realistic impairments: actually, it is assumed in [9] a perfect knowledge of all the parameters involved in the mixture. Moreover, the method performs well only if the residual f_{ru}, delays τ_u and phases ϕ_u are null which does not hold in practice. This method does not meet our constraints either.

C. AMPT: a natural choice for efficient MAMC

We finally justify the use of Analytical Mth-Power nonlinear Transformation for MAMC in the blind co-channel context.

Note that the assumptions related to timing and frequency imply that we are operating in one of the most challenging MAMC case study. In fact, if the T_u were different, CM/CC based methods would work successfully, as in [10]. In the case of partially overlapping signals – i.e. when the residual CFOs are of the order the symbol rhythm – filter-bank may be use to separate the interferers before the AMC step [9]. However, to the best of our knowledge, the realistic scenario proposed in Section II has never been specifically carried out.

1) A strong relation with Cyclostationarity-based methods: Cyclic Moments (CM) and Cyclic Cumulants (CC) seem the most promising in the blind multiuser context for their robustness to Carrier Frequency Offsets (CFO), Phase Offsets and Time Offsets [18] that inherently exist in the mixture. As a consequence, no intricate demodulation step is needed and the AMC is almost directly performed on the received signal.

The Cyclic Moment of y is especially defined as

$$R_y^{\alpha}(\boldsymbol{\tau})_{n,q} = \int_{-\infty}^{\infty} \prod_{i=1}^{n} y^{(*)_i}(t+\tau_i) e^{-i2\pi\alpha t} dt \qquad (6)$$

where n is the order and $(*)_i$ represents the q conjugations.

In the literature, n^{th}-order/q-conjugated CMs with $q = n/2$ are classically used to generate features which are for instance robust to phase noise [23]. With such a transform, a strong spectral line appears at each multiple of the cyclic-frequency.

In the presence of multiple co-channel signals, it is mandatory to choose $q \neq n/2$ so that the features will not overlap in the cyclic spectral space. As further defined in Section IV, the MPT of y may be seen as a derivative of the CM of y with $n = M$, $q = 0$ and $\boldsymbol{\tau} = \mathbf{0}$.

2) MPT-based AMC in the literature: The use of MPT for "classical" AMC was first proposed in [24] and recently applied in the Compressed Sensing context [25]. An improved version was also studied in [11] to distinguish between PSK, QAM and "hybrid" constellations. Thereby, it was proposed to base the recognition on the theoretical power of the generated spectral lines – through a method called AMPT – and not only on their cardinality. In fact, the fusion of these features for several M proved to provide stronger statistics for the classification. In the present work, we generalize the AMPT-based AMC to co-channel mixtures: the further theoretical developments lead us to a practical blind MAMC algorithm.

3) A moderate complexity: Since MAMC shows a practical interest in embedded Smart Modems, the complexity matters. MPT-based MAMC relies on the computation of a few PSDs, which complexity is of the order of the FFT. The complexity of the other processing blocs is mainly due to numerical methods on scalars (Section XIII) and they are in practice negligible.

Compared to the existing literature, the proposed method is slightly less complex than the Cyclic-Cumulants-based MAMC in [10]. However, AMPT-based method is more complex than [9] (relying on Classical Cumulants which are low-complexity) but as seen the blind performance results (Section IX), the trade-off is clearly in favor of our method.

IV. Basics on M^{th}-Power nonlinear Transform

In the scope of this article, we define the M^{th}-Power Transform of y, denoted as $M\text{PT}_y(f)$, as the M^{th}-root of the Power Spectral Density (PSD) of $y^M(t)$. Then we have

$$M\text{PT}_y(f) \triangleq \left|\mathcal{F}\left(y^M(t)\right)(f)\right|^{\frac{2}{M}}, \tag{7}$$

where $\mathcal{F}(\cdot)(f)$ stands for the classical Fourier Transform (FT).

As we will further see, the M^{th}-root is not necessarily required, but it nonetheless allows the power of the extracted features to be comparable when several values of M are used. Then, the M^{th}-root is preferred for a better fusion of the features in the Minimum Distance (MD) sense. However, in the case of a hierarchical tree-based classification, the M^{th}-root is not needed since the features are compared with precomputed thresholds instead of with one another.

Also remark that the discrete-time model has to be considered in practice: the MPT of $y(n)$ – where n is the time index – is practically performed thanks to the classical Discrete-Time Fourier Transform (DTFT). Then, as exposed in [11], the MPT is computed from discrete-time signal $y(n)$ according to

$$M\text{PT}_y(f) = N_e{}^{-\frac{2}{M}} \cdot \left|\sum_{n=0}^{N_e-1} y^M(n) \cdot e^{-2i\pi nf/N_e}\right|^{\frac{2}{M}}, \tag{8}$$

where we recall that N_e stands for the number of samples.

In the next Section, we derive the analytical expression of the power and position of the spectral lines occurring in the MPT function in the single-signal scenario. These results are then extended to the co-channel interference context – i.e. for $U > 1$ (almost)-totally overlapping signals – in Section VI.

V. Spectral lines in the single-signal context

In this section, we derive the theoretical power of the spectral lines generated by the MPT functions (7) with a single-signal (i.e. when $U = 1$). These powers – jointly taken with their respective spectral positions – represent the features that are further exploited to classify the incoming constellation.

A. Theoretical power of the spectral lines

We assume that $y(t)$ is a continuous noise-free infinite-length signal, whose discretized version is given by (4). For the sake of coherence with Section VI, we keep index u in the following notation so that $y_u(t) = y(t)$.

The MPT function is not affected by residual phases and delays as proposed in [25]. For conciseness, these parameters are both set to 0 without any loss of generality. It is obvious that residual CFO f_{ru} shifts the spectral line by $M \cdot f_{ru}$, while amplitude a_u multiplies its power by a_u^2. For ease of notation, we set f_{ru} to 0 and a_u to 1 in what directly follows.

First, we develop the general literal expression of continuous time signal $y_u(t)$ raised to power M (please refer to Appendix A for further justification of these results). Starting with

$$y_u^M(t) = \left(\sum_{k\in\mathbb{Z}} s_u(k) \cdot h_u\left(t - k \cdot T\right)\right)^M, \tag{9}$$

and following the work in [16], $y_u^M(t)$ is fully written as

$$y_u^M(t) = \sum_{\mathbf{i}\in\mathcal{I}_M} \binom{M}{\mathbf{i}} y_{u,\mathbf{i}}(t), \tag{10}$$

where, in (10), the following notation was adopted:

$$\mathcal{I}_M = \left\{\mathbf{i} \in \mathbb{Z}^M, \sum_{j=1}^{M} i_j = M, i_k{=}0 \implies \forall k' \geq k, i_{k'}{=}0\right\}, \tag{11}$$

$$\binom{M}{\mathbf{i}} \triangleq \frac{M!}{\prod_{j=1}^{M}(i_j!)}, \tag{12}$$

$$y_{u,\mathbf{i}}(t) = \sum_{\mathbf{k}\in\mathcal{K}_M^{\mathbf{i}}} \prod_{j=1}^{M} s_u^{i_j}(k_j) \cdot h_u^{i_j}\left(t - k_j \cdot T\right), \tag{13}$$

and where, in (13), we have

$$\mathcal{K}_M^{\mathbf{i}} = \left\{\mathbf{k} \in \mathbb{Z}^M, \begin{bmatrix} k_j{=}0 \text{ if } i_j{=}0 \\ i{<}j \implies k_i{<}k_j \text{ else} \end{bmatrix}\right\}. \tag{14}$$

In (10), some terms in the right-hand side sum are such that $\mathbb{E}\left[y_{u,\mathbf{i}}(t)\right] \neq 0$. The presence of a spectral line at each frequency which is a multiple of the symbol rhythm is made obvious according to the Poisson Summation Formula, since

$$\mathbb{E}\left[y_{u,\mathbf{i}}(t)\right] = \frac{1}{T} \sum_{\mathbf{k}\in\mathcal{K}_M^{0\mathbf{i}}} \mu_{u,\mathbf{k}}^{\mathbf{i}} \sum_{m\in R\mathbb{Z}} e^{i\cdot mt} \cdot H_{u,\mathbf{k}}^{\mathbf{i}}(m), \tag{15}$$

where we denoted

$$\mathcal{K}_M^{0\mathbf{i}} = \left\{\mathbf{k} \in \mathcal{K}_M^{\mathbf{i}} \text{ s.t. } k_1 = 0\right\}, \tag{16}$$

$$\mu_{u,\mathbf{k}}^{\mathbf{i}} = \mathbb{E}\left[\prod_{j=1}^{M} s_u^{i_j}(k_j)\right], \tag{17}$$

$$H_{u,\mathbf{k}}^{\mathbf{i}}(f) = \mathcal{F}\left(\prod_{j=1}^{M} h_u^{i_j}\left(t - k_j \cdot T\right)\right). \tag{18}$$

From (7), (10) and (15), we deduce the analytical power of the spectral line generated by $M\text{PT}_{y_u}$ around null frequency. We denote this power $\lambda_{u,M}$, whose analytical expression is

$$\boxed{\lambda_{u,M} = \left|\frac{1}{T}\sum_{\mathbf{i}\in\mathcal{I}_M} \binom{M}{\mathbf{i}} \cdot \sum_{\mathbf{k}\in\mathcal{K}_M^{0\mathbf{i}}} \mu_{u,\mathbf{k}}^{\mathbf{i}} \cdot H_{u,\mathbf{k}}^{\mathbf{i}}(0)\right|^{\frac{2}{M}}} \tag{19}$$

As we can see, several terms participate to the theoretical power of this spectral line. In fact, for a given M and for a transmitted constellation C_u, some specific couples of vectors $(\mathbf{i}, \mathbf{k})$ are such that neither $\mu_{u,\mathbf{k}}^{\mathbf{i}}$ nor $H_{u,\mathbf{k}}^{\mathbf{i}}(0)$ is null.

Theoretical expression of $\mu_{u,\mathbf{k}}^{\mathbf{i}}$ can be obtained from the i^{th}-order moment $\mu_u^{(i)}$ of the emitted constellation C_u under the $i.i.d.$ hypothesis for the source symbols. We actually have

$$\mu_{u,\mathbf{k}}^{\mathbf{i}} = \prod_{j=1}^{M} \mathbb{E}\left[s_u^{i_j}(k_j)\right] = \prod_{j=1}^{M} \mu_u^{(i_j)} = \mu_u^{\mathbf{i}}. \tag{20}$$

Some values of $\mu_u^{(i)}$ are tabulated in Table II for the constellations considered thereby. For odd values of M, the moments are all null and they have been willingly removed.

Meanwhile, obtaining an analytical expression for $H_{u,\mathbf{k}}^{\mathbf{i}}(0)$ is quite tedious for the pulse-shaping functions classically considered – such as the root-raised cosine filter used thereby.

TABLE II
THEORETICAL i^{th}-ORDER MOMENTS $\mu_u^{(i)}$ FOR $C_u \in \mathcal{C}$

Mod. $\rightarrow$	BPSK	QPSK	8PSK	8AMPM	R8QAM	16QAM
$\mu_u^{(2)}$	1	0	0	$-\frac{1}{5}$	$\frac{2}{3}$	0
$\mu_u^{(4)}$	1	1	0	$\frac{17}{25}$	$\frac{1}{3}$	$-\frac{17}{25}$
$\mu_u^{(6)}$	1	0	0	$-\frac{241}{125}$	$-\frac{22}{27}$	0
$\mu_u^{(8)}$	1	1	1	$\frac{1377}{625}$	$-\frac{263}{81}$	$\frac{1377}{625}$

In practice, for a given radio standard, we would numerically compute $H^{\mathbf{i}}_{u,\mathbf{k}}(0)$ and store it for different sets of parameters.

As an example and in order to illustrate the behaviour of (19), we develop in the next two subsections the simplified expression of $\lambda_{u,M}$ for $M = 2$ and $M = 4$.

B. Simplified expression of $\lambda_{u,M}$ for $M = 2$

As previously proposed, $y_u^2(t)$ easily splits into two sums:

$$y_u^2(t) = y_{u,20}(t) + 2 \cdot y_{u,11}(t), \tag{21}$$

where

$$\begin{cases} y_{u,20}(t) = \sum_{k_1} s_u^2(k_1) \cdot h_u^2\left(t - k_1 T\right) \\ y_{u,11}(t) = \sum_{k_1 < k_2} s_u(k_1) s_u(k_2) \cdot h_u(t - k_1 T)\, h_u(t - k_2 T) \end{cases}$$

Term $y_{u,20}(t)$ may show a spectral line if $\mathbb{E}\left[s_u^2\right] \neq 0$, which is true for non-$\pi/2$-rotation-invariant constellations such as BPSK or R8QAM. However, with $i.i.d.$ symbols, $\mathbb{E}[s_u(k_1)s_u(k_2)] = 0$ whatever C_u and no spectral line occurs.

If we consider that h_u is a square-root raised cosine filter and whatever the roll-off β_u, we eventually get $H^{20}_{u,\mathbf{0}}(0) = T$. Then, in this context, the analytical expression of $\lambda_{u,2}$ is

$$\lambda_{u,2} = \left| \frac{1}{T} \cdot \left(\mu_u^{(2)} \cdot T + 0 \cdot \sum_{k>0} H^{11}_{u,0k}(0) \right) \right| = \left| \mu_u^{(2)} \right|. \tag{22}$$

C. Simplified expression of $\lambda_{u,M}$ for $M = 4$

Likewise, the theoretical expression of $\lambda_{u,4}$ is drawn in the same context. Now, several terms in the development of y_u^4 contribute to the power of the spectral line. Herein, we get

$$y_u^4 = y_{u,4000} + 16 y_{u,3100} + 6 y_{u,2200} + 36 y_{u,2110} + 24 y_{u,1111}. \tag{23}$$

Among the right-hand side terms in (23), only $y_{u,4000}$ and $y_{u,2200}$ may show a non-null expectation and contribute to the power of the spectral line. Meanwhile, terms $y_{u,3100}$, $y_{u,2110}$ and $y_{u,1111}$ show null expectations: they have no effect on the power of the spectral line whatever the constellation.

The development of theoretical $\lambda_{u,4}$ according to (19) is a bit more tedious than for $M = 2$ but follows the exact same principle. We eventually get after some simplifications

$$\lambda_{u,4} = \left| \frac{1}{T} \left(\mu_u^{(4)} H^{4000}_{u,\mathbf{0}}(0) + 6 \left(\mu_u^{(2)} \right)^2 \sum_{k>0} H^{2200}_{u,0k00}(0) \right) \right|^{\frac{1}{2}}. \tag{24}$$

No simple analytical formulas were found neither for $H^{4000}_{u,\mathbf{0}}(0)$ nor for $H^{2200}_{u,0k00}(0)$ in the situation where h_u is a square-root raised cosine (SRRC) filter. Anyway, these values are numerically computable and they can be tabulated to further reduce the complexity of the classification algorithm.

VI. SPECTRAL LINES IN THE CO-CHANNEL CONTEXT

We now consider the co-channel interference scenario: to this end, we adopt the assumptions proposed in Section II. To develop the analytical expression of the power and position of the spectral lines, we first consider that the mixture is composed of U continuous-time and free of noise signals.

A. Preliminary considerations

By expanding the M^{th}-power of the received mixture of U signals according to the multinomial theorem, we get

$$y^M(t) = \sum_{\mathbf{m} \in \mathcal{M}_U^M} \binom{M}{\mathbf{m}} \prod_{u=1}^{U} y_u^{m_u}(t), \tag{25}$$

where $\mathbf{m} = (m_1, \cdots, m_U)$, where the multinomial coefficients are classically developed as in section V as

$$\binom{M}{\mathbf{m}} \triangleq \frac{M!}{\prod_{u=1}^{U} m_u!}, \tag{26}$$

and where $\mathcal{M}_U^M$ denotes the following set:

$$\mathcal{M}_U^M = \left\{ \mathbf{m} = (m_1, \cdots, m_U) \in \mathbb{N}^U, \sum_{u=1}^{U} m_u = M \right\}. \tag{27}$$

B. Cardinality of the set of spectral lines for a given M

Some right-hand side terms of the sum in (25) may produce a spectral line. In what follows, we derive the expression of the subsets of $\mathcal{M}_U^M$ prone to generate spectral lines, mainly depending on the set of constellations $\{C_u\}$.

Let first remark that all zero-mean π-rotational symmetric constellations don't produce any spectral line if at least one of the m_u is odd. Thus, for usual constellations such as the one considered in the scope of this article, the sum in (25) is performed on the following reduced set whatever $\{C_u\}_{u \in \{1,\cdots,U\}}$:

$$\mathcal{M}_U^{M,\mathbf{2}} = \left\{ \mathbf{m} \in \mathcal{M}_U^M \cap (2\mathbb{N})^U \right\}, \tag{28}$$

which can be formulated using the notation of (27) as

$$\mathcal{M}_U^{M,\mathbf{2}} = 2 \cdot \mathcal{M}_U^{M/2}. \tag{29}$$

The number of terms in the sum in (25) participating to the theoretical power of the spectral lines that may appear in the MPT of y is the cardinality of $\mathcal{M}_U^{M/2}$. This set is known, in combinatorics, as the set of all the $M/2$-multicombinations [26]. The cardinality of this set for $U \geq 1$ is expressed as

$$\text{Card}\left(\mathcal{M}_U^{M/2} \right) = \left(\!\!\binom{U}{M/2}\!\!\right), \tag{30}$$

where $(\!(\cdot)\!)$ – reads "U multichoose $M/2$" – is analytically given in terms of classical combinations and for $U \geq 1$ as

$$\left(\!\!\binom{U}{M/2}\!\!\right) = \binom{U + M/2 - 1}{M/2}. \tag{31}$$

We finally get the number of expected spectral lines around the null frequency for a given $\{M, U\} \in \mathbb{N}^{*2}$,

$$\text{Card}\left(\mathcal{M}_U^{M,\mathbf{2}} \right) = \frac{(U + M/2 - 1)!}{(U-1)! \cdot (M/2)!}. \tag{32}$$

Some values of Card$\left(\mathcal{M}_U^{M,\mathbf{2}}\right)$ for small values of M and U are gathered in Table III:

TABLE III
TYPICAL VALUES OF CARD $\left(\mathcal{M}_U^{M,\mathbf{2}}\right)$ FOR SOME M AND U

$M\downarrow \quad U\rightarrow$	1	2	3	4	5
2	1	2	3	4	5
4	1	3	6	10	15
6	1	4	10	20	35
8	1	5	15	35	70

Note that it is still possible to refine the set given by (28) when considering the order of the rotational symmetry of the emitted constellations. Actually, as this order grows, some standard moments of the constellation become null and some spectral lines do no longer appear. Then, if we assume that C_u is $2\pi/X_u$-rotational symmetric – with X_u the highest possible – then the sum in (25) is performed on reduced set

$$\mathcal{M}_U^{M,\mathbf{X}} = \left\{\mathbf{m} \in \mathcal{M}_U^M \cap \mathbf{X}\mathbb{N}\right\}. \tag{33}$$

The analytical formula of Card$\left(\mathcal{M}_U^{M,\mathbf{X}}\right)$ whatever $\mathbf{X}$, U and M is rather inconvenient and proves not to be crucial. Instead, we assume that the number of spectral lines is always given by (32) whatever the emitted constellations. However, some spectral lines may appear with a null power.

C. Analytical power of the spectral lines

Following the previous development, it is possible to derive the theoretical power of each term in the sum in (25). In fact, for a given vector $\mathbf{m}$, we may get (see Appendix B.)

$$\boxed{\lambda_{\mathbf{m}} = \left(\frac{M!}{\prod_{u=1}^{U} m_u!} \cdot \prod_{u=1}^{U} \left(a_u^2 \cdot \lambda_{u,m_u}\right)^{\frac{m_u}{2}}\right)^{\frac{2}{M}}}, \tag{34}$$

where, as defined previously, λ_{u,m_u} stands for the theoretical power of the spectral line generated by $y_u^{m_u}$ if it was alone.

Formula (34) is of major interest since it shows that the theoretical powers of the spectral lines in the interfering case can simply be derived from the ones in the single-signal case.

D. Position of the spectral lines

Let us now consider the spectral shift entailed by the residual carrier frequencies f_{ru} on the spectral lines. While replacing y_u in (25) by its expression, literally given by (5), it is straightforward that the spectral line generated for a given $\mathbf{m}$ simply appears at frequency $f_{\mathbf{m}}$, such that

$$f_{\mathbf{m}} = \sum_{u=1}^{U} m_u \cdot f_{ru}. \tag{35}$$

Similarly to the way we normalize the power of the spectral lines – as the M^{th}-root of the PSD – we define the normalized spectrum scale f' such that $f' = \frac{f}{M}$. Then, the normalized position of the spectral line indexed by vector $\mathbf{m}$ is

$$f'_{\mathbf{m}} \triangleq \frac{1}{M} \sum_{u=1}^{U} m_u \cdot f_{ru}. \tag{36}$$

E. Theoretical features for a mixture of two signals

According to the previous development, we gathered in Table IV the expected number, powers and positions of the spectral lines for a few values of M when $U = 2$.

TABLE IV
PROPERTIES OF THE FEATURES FOR A MIXTURE OF 2 SIGNALS

$M\downarrow$	Peaks	Norm. $f'_{\mathbf{m}}$	Theoretical Power $\lambda_{\mathbf{m}}$
2	2	f_{r1}, f_{r2}	$a_1^2\lambda_{1,2}, a_2^2\lambda_{2,2}$
4	3	$f_{r1}, \frac{f_{r1}+f_{r2}}{2}, f_{r2}$	$a_1^2\lambda_{1,4}, a_1a_2\sqrt{6\lambda_{1,2}\lambda_{2,2}}, a_2^2\lambda_{2,4}$
6	4	$f_{r1}, \frac{2f_{r1}+f_{r2}}{3}$, $\frac{f_{r1}+2f_{r2}}{3}, f_{r2}$	$a_1^2\lambda_{1,6}, \sqrt[3]{15a_1^4a_2^2\lambda_{1,4}^2\lambda_{2,2}}$ $\sqrt[3]{15a_1^2a_2^4\lambda_{1,2}\lambda_{2,4}^2}, a_2^2\lambda_{2,6}$

In order to verify the proposed analytical development, we jointly represent, Fig. 6, the theoretical $\lambda_{\mathbf{m}}$ computed according to Table IV and the MPT functions of normalized $y(n)$ for a few M. Thereby, a mixture of a two signals was considered, respectively with constellations BPSK and R8QAM, and residual CFOs of -20 Hz and +40 Hz. The Signal-to-Interferer Ratio (SIR) of the strongest signal is 3.5 dB. The noise-free mixture was up-sampled by a factor $\rho = 4$ and N_e was set to $4 \cdot 10^5$ samples (which is high enough to verify the "infinite-length" observation hypothesis).

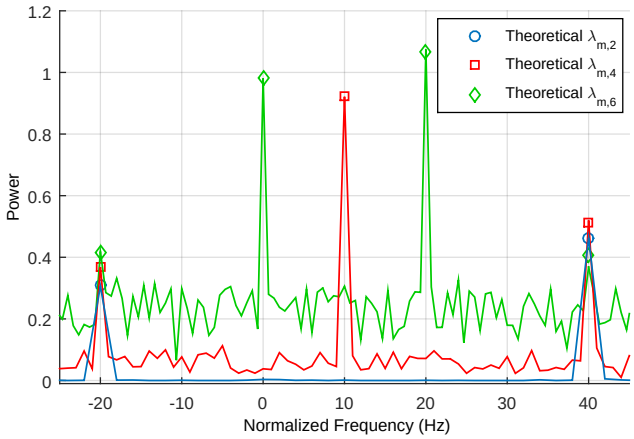

Fig. 6. Theoretical power $\lambda_{\mathbf{m}}$ and simulated $M\text{PT}_y(f')$

As expected, the theoretical position $f'_{\mathbf{m}}$ and power $\lambda_{\mathbf{m}}$ of each spectral line in the MPT matches the simulated ones.

F. Towards the noisy discrete-time finite-length model

Up to now, we considered the theoretical references obtained for continuous-time, infinite-length, noise-free signals. With noisy mixtures and small observation lengths, the power of the spectral lines is no longer deterministic and the spectral noise becomes quite substantial. In Section VII, we derive the Probability Density Functions (PDFs) for both the spectral lines and the background noise. This development aims at:

- Analytically derive the references in this realistic context.
- Get the theoretical probabilities of good detection of the spectral lines and false alarm rate in the blind scenario.
- Compute the theoretical Correct Classification Rate (CCR) in various AMC and MAMC scenarios.

VII. Probabilistic considerations

In this Section, we consider the effects of a noisy discrete-time finite-length model for the received signal, namely:

- The spectral background noise power impact on the power of the spectral lines.
- The statistical behaviour of the power of both the background noise and the spectral lines.

A. Motivation and preliminaries

Mazo rightly pointed out the first effect in [16]: performing the MPT computation on a finite-length signal inherently leads to the integration of the background noise in a bandwidth of size $\frac{f_e}{N_e}$ around $f_{\mathbf{m}}$. The mean background noise quickly increases with both M and U and decreases with the composite SNR, which motivates to study its impact on measured $\widehat{\lambda}_{\mathbf{m}}$. Mazo proposed a general framework to compute the mean background noise power, based on the expression of the PSD as the Fourier Transform of the autocorrelation function of y. While this method is easy to apply for $M = 2$ and $U = 1$ – which was done by Reichert in [24] for Gaussian filters – it becomes infeasible for higher values of M and U due to the exponentially growing number of cross terms appearing in the autocorrelation function of y. Besides, it does not give any information on the distributions of the spectral power, which is needed to unfold the analytical expression of both the good detection and false alarm rates in the blind scenario.

Instead, we propose to draw the PDFs of the spectral power by considering that the mean background noise power around the spectral lines in $(M\text{PT}_y)^M(f)$, denoted by η_M, is easily estimable. Following [24], we may consider the probabilistic distributions under two different hypothesis, namely:

- H_0 – $M\text{PT}_y(f)$ belongs to the background noise
- H_1 – $M\text{PT}_y(f)$ is a spectral line.

B. Distribution of the power of the background noise (H_0)

It can be shown that the probabilistic behaviour of $(M\text{PT}_y)^M(f)$ under hypothesis H_0 follows a centered chi-squared distribution with two degrees of freedom – see e.g., [24] [27] [28]. Then, the PDF for each frequency bin around the null frequency and under hypothesis H_0 is derived as

$$p\left[M\text{PT}_y^M(f) = x|H_0\right] = \frac{1}{\eta_M} \cdot e^{-\frac{x}{\eta_M}}, \tag{37}$$

where we recall that η_M stands for the mean background noise power surrounding the spectral lines. η_M is given by

$$\eta_M = \left\langle M\text{PT}_y^M(f) \right\rangle_{f \in B_M}, \tag{38}$$

where B_M is such that for all f in B_M, $M\text{PT}_y(f)$ shows no spectral line and is almost identically distributed. This second assertion is true when f is close to the null frequency. Note that "$< \cdot >$" classically stands for the mean value.

C. Distribution of the power of the spectral lines (H_1)

Deriving the PDF for the spectral lines is also needed to get the analytical expression of the references. It also allows to get the theoretical probability of good detection of the spectral lines and the Correct Classification Rate (CCR) of the (M)AMC method with a Minimum Distance classifier.

The power of $(M\text{PT}_y)^{M/2}(f_{\mathbf{m}})$ proves to follow a Rice distribution [24]. Equivalently, $(M\text{PT}_y)^M(f_{\mathbf{m}})$ follows a non-central Chi-squared distribution with 2 degrees of freedom:

$$p\left[M\text{PT}_y^M(f_{\mathbf{m}}) = x\right] = \frac{1}{\eta_M} \cdot e^{-\frac{x+\lambda_{\mathbf{m}}^M}{\eta_M}} \cdot I_0\left(\frac{2\sqrt{x\lambda_{\mathbf{m}}^M}}{\eta_M}\right), \tag{39}$$

where $I_0(\cdot)$ stands for the modified Bessel function of the first kind with order zero. From (39), we get (see Appendix C.)

$$p\left[M\text{PT}_y(f_{\mathbf{m}}) = x\right] = \frac{Mx^{M-1}}{\eta_M} \cdot e^{-\frac{x^M+\lambda_{\mathbf{m}}^M}{\eta_M}} \cdot I_0\left(\frac{2\sqrt{x^M\lambda_{\mathbf{m}}^M}}{\eta_M}\right). \tag{40}$$

D. References in the discrete-time finite-length context

Based on the above development, the references $\lambda_{\mathbf{m}}^{ref}$ used to compare the constellations in the Minimum Distance (MD) sense can be analytically developed has the expected value of the distribution of the power of the spectral line (40), yields

$$\lambda_{\mathbf{m}}^{ref} = \sqrt[M]{\eta_M} \cdot e^{-\frac{\lambda_{\mathbf{m}}^M}{\eta_M}} \cdot \Gamma\left(1+\frac{1}{M}\right) \cdot {}_1F_1\left(1+\frac{1}{M}, 1, \frac{\lambda_{\mathbf{m}}^M}{\eta_M}\right), \tag{41}$$

where Γ stands for Euler's Gamma function and ${}_pF_q\left(a, b, x\right)$ the p, q-order generalized hypergeometric function.

We may remark that if $\lambda_{\mathbf{m}}^M$ is large compared to η_M, then the following approximation holds:

$${}_1F_1\left(1+\frac{1}{M}, 1, \frac{\lambda_{\mathbf{m}}^M}{\eta_M}\right) \simeq \frac{e^{\frac{\lambda_{\mathbf{m}}^M}{\eta_M}}}{\Gamma\left(1+\frac{1}{M}\right)} \cdot \left(\frac{\lambda_{\mathbf{m}}^M}{\eta_M}\right)^{\frac{1}{M}}. \tag{42}$$

Then, $\lambda_{\mathbf{m}}^{ref} \simeq \lambda_{\mathbf{m}}$. In other words, the PDF given by (40) is almost centred around $\lambda_{\mathbf{m}}$. In that case, it is not mandatory to use (41) to refine the references and using the expression given by (34) gives sufficient precision for the references.

E. Blind detection of the Spectral Lines

In the blind context, the first step is to detect the spectral lines in the computed $(M\text{PT}_y)^M$ functions. The probability of detecting a false spectral line at a given frequency f with threshold ξ_M is derived according to (37) as

$$P_{F,s,M} = \int_{\xi_M}^{+\infty} \frac{1}{\eta_M} \cdot e^{-\frac{x}{\eta_M}} dx = e^{-\frac{\xi_M}{\eta_M}}. \tag{43}$$

The detection of the spectral lines can be handled on a reduced part of the spectrum: this set is centered around 0 and its bounds mainly depend on the maximum expected value of the CFOs. If we assume that the maximum normalized CFO for all the users is $\pm f_{max}$, then the peak detection is performed on $n_b = 2MN_e f_{max}$ frequency bins. Moreover, the power of the background noise bins proves to be identically distributed in $[-f_{max}; f_{max}]\backslash\{f_{\mathbf{m}}\}$ if $f_{max} << T^{-1}$. Then, we get the following false alarm rate in the considered bandwidth:

$$P_{F,M} \simeq 1 - \left(1 - e^{-\frac{\xi_M}{\eta_M}}\right)^{n_b}. \tag{44}$$

Fig. 7 shows the theoretical probability of false detection on the whole spectrum-of-interest (44) and the simulated one for $M = \{2, 4\}$. Here, n_b was set to $50M$, U to 2, ρ to 4, N_e to $4 \cdot 10^4$ and SNR to 10 dB. These probabilities are represented as a function of the normalized threshold ξ_M/η_M.

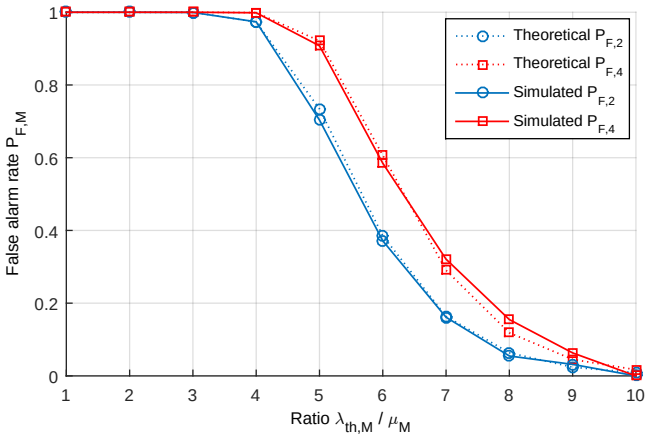

Fig. 7. Theoretical and simulated false alarm rates $P_{F,2}$ and $P_{F,4}$

From (44), we get the expression of ξ_M for a given $P_{F,M}$:

$$\xi_M \simeq -\eta_M \cdot \ln\left(1-(1-P_{F,M})^{\frac{1}{n_b}}\right). \tag{45}$$

Generally – mainly to get the least possible outliers and have a simple post-processing algorithm – we choose ξ_M such that $P_{F,M}$ is as small as possible while correctly detecting most of the spectral lines. For a given ξ_M, the probability of good detection of the spectral line occurring at frequency $f_{\mathbf{m}}$ is derived using the Cumulative Distribution Function (CDF) of the non-central Chi-squared distribution. We may get:

$$P_{D,\mathbf{m}} = Q_1\left(\sqrt{\frac{2\lambda_{\mathbf{m}}^M}{\eta_M}}, \sqrt{\frac{2\xi_M}{\eta_M}}\right) \tag{46}$$

where $Q_1(\cdot,\cdot)$ stands for the first-order Marcum Q-function.

VIII. Blind MAMC based on AMPT

Throughout this section, we propose to blindly solve the inverse problem of estimating parameters U and $\{f_{ru}, a_u, C_u\}_{u\in\{1,\cdots,U\}}$, given functions $M\text{PT}_y$ for some M.

A. General scheme of the proposed blind MAMC method

We first draw the block diagram of the whole method with the references to specific equations or algorithms in Fig. 8.

B. Preprocessing Unit

As previously discussed, the preprocessing unit transforms the incoming signal $x(n)$ into a normalized, pseudo-centred and pre-filtered signal $y(n)$. For instance, this step can be performed according to the method proposed in [11].

The preprocessing unit also estimates some parameters of the mixture if needed, such as the oversampling factor ρ.

C. Detection of the spectral lines in the MPTs

The decision starts with the detection of the spectral lines in the computed MPTs. As stated in Section VII, proper threshold ξ_M has to be chosen to find a compromise between the good detection rate and the false-alarm rate. We propose – with Algorithm 1. – to detect the spectral lines with a chosen false-alarm rate $P_{F,M}$. The spectral lines are then sorted by decreasing Peak-to-Background Noise Ratio (PBNR).

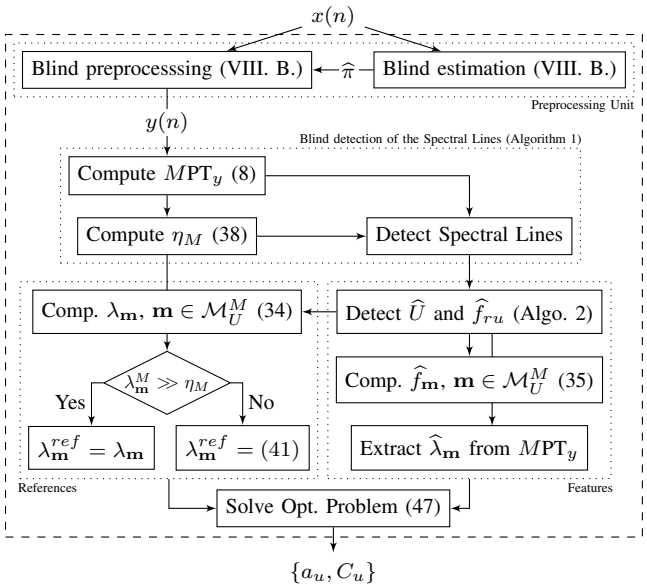

Fig. 8. The proposed AMPT-based blind MAMC algorithm

Algorithm 1 Constant false-alarm rate detector for set $\{M\}$

1: For each M, compute the $M\text{PT}_y^M(f)$ with function (8)
2: For each M, compute η_M (38)
3: For each M, set ξ_M for a chosen $P_{F,M}$ (45)
4: Detect the spectral lines, sort them by decreasing PBNR

D. Computation of the features $\widehat{\lambda}_{\mathbf{m}}$

Thereby, we develop the method to compute the features $\widehat{\lambda}_M$ for some M. This task is not an issue when the number of users U and the residual carrier frequencies f_{ru} are known. In this situation, we simply compute the powers given by (8) for each $f_{\mathbf{m}}$ (35) such that $\mathbf{m}$ is in $\mathcal{M}_U^{M,\mathbf{2}}$ (28).

In the blind scenario, U and the residual CFOs f_{ru} are not known. Then, we have to estimate them to correctly run the computation of the features.

To proceed, we propose an algorithm which iteratively builds a basis $\{\widehat{f}_{ru}\}$ and estimate $\widehat{U}$ based on the set of detected spectral lines. We first work on the spectral lines that show high PBNRs to make the construction robust to outliers and to forgotten spectral line.

On overview of the method is proposed in Algorithm 2. We denote by n_{SL} the number of spectral lines detected with Algorithm 1. The n^{th} spectral line is represented by its frequency f_n and the order M_n of the MPT. $\mathbf{F}_n$ represents the frequency basis obtained with the n first spectral lines.

Algorithm 2 Estimation of $\widehat{U}$ and $\{\widehat{f}_{ru}\}$ by decreasing PBNR

1: Initialize $\mathbf{F}_0 = \emptyset$ and $\widehat{U} = 0$
2: **for** $n = 1 : n_{SL}$ **do**
3: **if** f_n is not a linear combination of $\mathbf{F}_{n-1}$ (35) **then**
4: $\widehat{U} \leftarrow \widehat{U} + 1$
5: $\mathbf{F}_{n-1} \leftarrow \mathbf{F}_{n-1} \cup f_n$
6: Find $\mathbf{F}_n$ by orthogonalizing $\mathbf{F}_{n-1}$
7: **end if**
8: **end for**

At the end of the algorithm, we get the estimated number of users $\widehat{U}$ and a basis $\mathbf{F}_{n_{SL}}$ – also denoted as $(\widehat{f}_1, \cdots, \widehat{f}_{\widehat{U}})$ – that describes the positions of the detected spectral lines. The computation of $\widehat{\lambda}_{\mathbf{m}}$ is straightforward using (8) and (35).

E. Computation of the references $\lambda_{\mathbf{m}}^{ref}$

Analytical expressions of the references may be obtained according to (19) and (34), and refined according to (41) if needed. Note that for small values of M and U and for medium to high SNRs, computing the references using (34) gives sufficient precision and greatly simplifies the algorithm in charge of estimating $\{a_u\}$ and $\{C_u\}$.

F. Finding $\{a_u\}$ and $\{C_u\}$ by solving an optimization problem

In the blind scenario, sets $\{a_u\}$ and $\{C_u\}$, for all u in $\{1, \cdots, U\}$ are unknown. Our goal is to estimate these parameters in the Minimum Distance (MD) sense.

1) Problem statement: We assume that the $\widehat{\lambda}_{\mathbf{m}}$ have been correctly computed for all $\mathbf{m} \in \mathcal{M}_U^{M,\mathbf{2}}$. Then, in the MD sense, we look for set $\{\widehat{a}_u, \widehat{C}_u\}$ such that

$$\{\widehat{a}_u, \widehat{C}_u\} = \underset{\substack{\{a_u, C_u\} \\ \text{s.t. } \begin{cases} a_1^2+\cdots+a_U^2=1 \\ (C_1,\cdots,C_U)\in\mathcal{C}^U \end{cases}}}{\arg\min} \sum_{\mathbf{m}\in\mathcal{M}_U^{M,\mathbf{2}}}^{M} \left(\widehat{\lambda}_{\mathbf{m}} - \lambda_{\mathbf{m}}^{ref}\right)^2, \quad (47)$$

where we recall that $\lambda_{\mathbf{m}}^{ref}$ stands for the references, computed according to (34) and refined with (41) if assumed necessary.

2) Splitting the optimization problem: Solving (47) is performed by splitting the optimization problem: for each possible set $\{C_u\} \in \mathcal{C}^U$, we first find $\{\widehat{a}_u\}$ such that

$$\{\widehat{a}_u\} = \underset{\{a_u\}, \|\mathbf{a}\|_2^2=1}{\arg\min} \sum_{\mathbf{m}\in\mathcal{M}_U^M}^{M} (\widehat{\lambda}_{\mathbf{m}} - \lambda_{\mathbf{m}}^{ref})^2 \quad (48)$$

Then, the set of constellations $\{\widehat{C}_u\}$ is the one which minimizes (47) according to the respective estimated sets of amplitudes $\{\widehat{a}_u\}$.

G. Specific case study: $U = 2$ with the $2/4$PT classifier

Among the co-channel scenarios, the situation where two signals coexist is encountered in several contexts such as in dual-satellite systems. This scenario was studied by Zaerin et al. in [9] with simplifying assumptions. In Section IX, we mainly study the performance of our method in this specific context and we confront it with Zaerin's method.

Then, with two co-channel signals inferred by a 2PT/4PT classifier and under the approximation $\lambda_{\mathbf{m}}^{ref} \simeq \lambda_{\mathbf{m}}$, the following multivariate polynomial $\mathcal{P}$ has to be minimized

$$\begin{aligned}\mathcal{P}(a_1, a_2) = &\left(\widehat{\lambda}_{20} - a_1^2\lambda_{1,2}\right)^2 + \left(\widehat{\lambda}_{02} - a_2^2\lambda_{2,2}\right)^2 + \\ &\left(\widehat{\lambda}_{40} - a_1^2\lambda_{1,4}\right)^2 + \left(\widehat{\lambda}_{22} - a_1 a_2\sqrt{6\lambda_{1,2}\lambda_{2,2}}\right)^2 + \left(\widehat{\lambda}_{04} - a_2^2\lambda_{2,4}\right)^2\end{aligned} \quad (49)$$

This problem is easily solved by neglecting the effects of the cross term – i.e. the fourth right hand side term in (49) – on the solution $\{\widehat{a}_1; \widehat{a}_2\}$ which minimizes (49). This last approximation leads to an analytical formula for $\{\widehat{a}_1; \widehat{a}_2\}$.

IX. Simulation Results

In this penultimate Section, we show the effectiveness of the proposed method throughout numerical simulations in various scenarios. To this end, this Section is split into three main subsections. The first part deals with the good detection rate of the number of signals and their respective CFOs, which is a crucial step in the blind scenario. Then, we expose some results in the dual-signals blind context through the Correct Classification Rate obtained with the proposed 2PT-4PT classifier. Last, the performance of the proposed method are compared with the one obtained with Zaerin's method [9].

Otherwise stated, we consider that all the assumptions proposed in Section II hold. All the mixed sources are pulse-shaped by Square-Root Raised Cosine (SRRC) filters with roll-off 0.25. We consider that the adjacent channels and the Gaussian noise that lay outside band B are perfectly rejected by a proper bandpass filter. The oversampling factor ρ is arbitrarily set to 4. The baud-rate R is set to 1e^6 symbols per second for all the sources. The residual CFOs are randomly and uniformly chosen in band $[-1; +1]$ kHz. Moreover, we use the classical definitions of the composite SNR: $\text{SNR}_{dB} = 10 \cdot \log_{10}(\frac{\sum_{u=1}^{U} P_u}{P_\nu})$, where P_u stands for the power of signal u and P_ν for the power of the noise.

A. Detection of the number of signals and the residual CFOs

We first consider the problem of detecting the number of signals U in the considered bandwidth as well as the respective residual CFOs of these signals. The good detection of these parameters is in fact mandatory for the classification algorithm to properly work. We have to mention that when U is correctly estimated, then the estimated residual CFOs are also correct.

Fig. 9 shows the Correct Detection Rate (CDR) of the number of users versus the composite SNR when the users transmit BPSK constellations with same powers. To this end, we use both 2PT and 4PT and we jointly run Algorithm 1 for the detection of the spectral lines, and Algorithm 2 for the estimation of U and $\{f_{ru}\}$. Thereby, 2e^3 symbols were used for the detection, and the ratio ξ_M/η_M was set to 10 so that the overall false alarm rate – i.e. in both 2PT/4PT – is 0.5%.

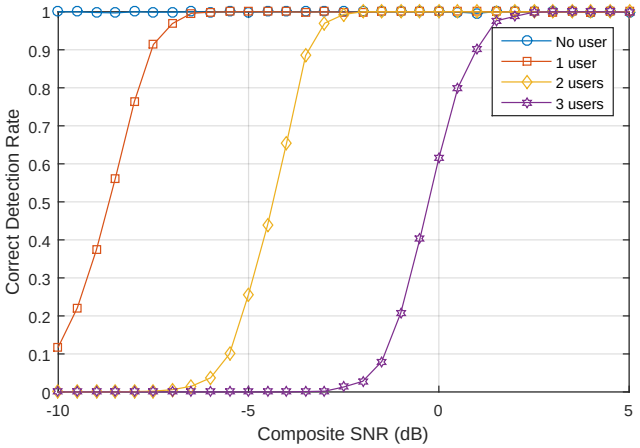

Fig. 9. Correct Detection Rate of the number U of overlapping BPSK signals as a function of the composite SNR, for $U \in \{0, 1, 2, 3\}$

B. 2PT/4PT-based blind MAMC with two co-channel signals

Thereby, we expose the performance of the whole proposed MPT-based MAMC for mixtures of two signals. Set $\mathcal{C}$ is composed of constellations BPSK, QPSK, 8AMPM, R8QAM and 16QAM for sufficient diversity in terms of SatComs.

First, Fig. 10 shows the Correct Classification Rate (CCR) arbitrarily for signal 1 when the Signal-to-Interferer Ratio (SIR) of both signals is equal to 0 dB. This scenario can be seen as a "worst case" in MAMC, as stated in [9].

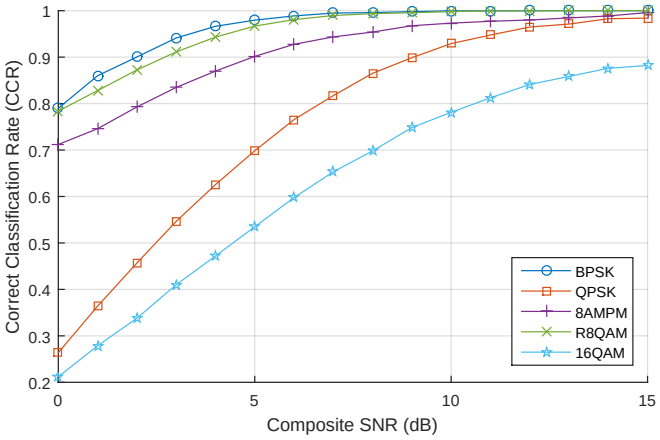

Fig. 10. Correct Classification Rate (CCR) for user 1 in the context of two overlapping signals – SIR = 0 dB – Blind scenario – N = $1e^4$

In Table V, we also expose the confusion matrix of the classifier in the same context as in Fig. 10 with SNR = 10 dB. Note that "0%" was replaced by " · " for a better readability.

		Emitted Constellation				
		BPSK	QPSK	8AMPM	R8QAM	16QAM
Classifier Output	BPSK	100%	.	.	.	.
	QPSK	.	92.8%	0.6%	.	17.4%
	8AMPM	.	1.8%	97.1%	.	4.5%
	R8QAM	.	.	.	100%	.
	16QAM	.	5.4%	2.3%	.	78.1%

TABLE V
CONFUSION MATRIX WITH $SNR = 10dB$ FOR THE PROPOSED 5-CLASS PROBLEM – SIR = 0 DB – BLIND SCENARIO – N = $1E^4$

As expected, the worst CCR is for both QPSK and 16QAM constellations since they are the closest in the 2PT/4PT feature-space. Meanwhile, the CCR for other types of constellation is satisfying even at low SNRs.

Last, Fig. 11 shows the mean CCR for both signals in the average realistic scenario, i.e. in the blind context and with a SIR randomly chosen in set $[0; 6]$ dB (signal 1 is assumed to be the strongest wlog). Other parameters are randomly chosen as previously stated. The mean performance is slightly better for BPSK, 8AMPM and R8QAM constellations, while an expected degradation of the CCR for QPSK and 16QAM is encountered. If considering a channel coded transmission with usual code rate, the CCR obtained at the minimum SNR allowing proper multiuser demodulation is truly acceptable.

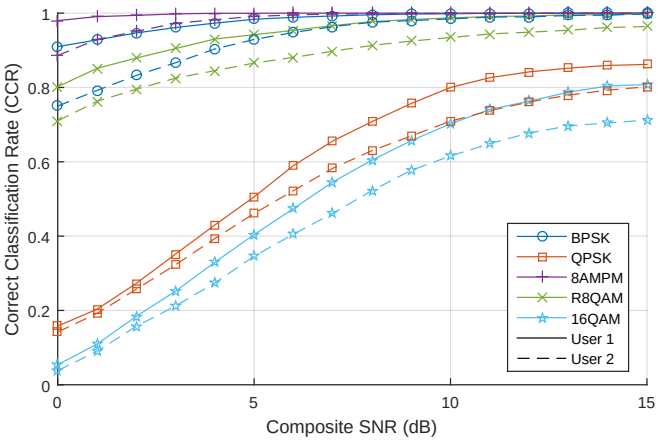

Fig. 11. Correct Classification Rate (CCR) for both signals in the context of two overlapping signals – SIR $\in [0; 6]$ dB – Blind scenario – N = $1e^4$

C. Comparison with Zaerin's MAMC method [9]

In this penultimate part, we propose to compare the MAMC method proposed in [9] with our 2PT/4PT-based classifier.

1) Preamble: Note that the method in [9] is the closest to the one we propose thereby. However, it is not designed for the blind situation and several strong assumptions are taken in the co-channel case. Especially, it is assumed that the signal is perfectly sampled at the symbol rhythm, which doesn't hold in practice. Moreover, the method is designed for rectangular pulse-shaping, for null CFO and with a perfect synchronisation between the interfering signals. Any offset, no matter how small, entails consequent degradations in the CCR. Instead, the method we propose is designed to handle these offsets and no degradation of the CCR is noticed.

To remain fair, we propose to compare both methods in the non-blind situation with no phase offset and no delay between the signals. However, we assume non-null residual CFOs when simulating both methods. We assume perfect synchronization for [9] while the over-sampling factor is set to 4 for the proposed AMPT-based method. Rectangular pulse-shaping is assumed for [9] while we use SRRC filters with roll-off 0.25 for the proposed AMPT-based method.

2) Simulation results: Fig. 12 shows the Correct Classification Rate (CCR) of both methods for a mixture of two signals when $\mathcal{C} = \{\text{BPSK, QPSK, 16QAM}\}$ and $N = 8000$.

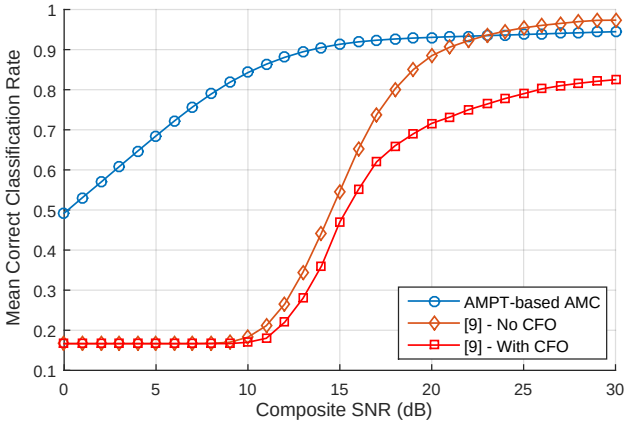

Fig. 12. Mean Correct Classification Rate for AMPT-based method and [9]

The proposed AMPT-based method clearly outperforms the method in [9], even in the context of perfectly synchronized signals. Moreover, note that the performance of the MAMC method in [9] would significantly drop with delays between the users or when the amplitudes of the signals are different.

X. Conclusion

We have proposed a new method for the blind modulation classification of co-channel overlapping signals in the cognitive satellite context. It is based on an Analytical study of the M^{th}-Power nonlinear Transformation (AMPT) of the mixture.

This method shows two main advantages. First, it makes no assumption regarding time and frequency synchronization at the receiver. Thus, no intricate demodulation scheme is needed and the constellation recognition is performed in a blind manner almost directly on the received signal. Secondly, its complexity is of the order of the Fourier Transform, which makes the whole algorithm feasible in cognitive receivers.

We showed that AMPT-based MD-sense classification was able de distinguish between several constellations even if they are very close to each other in the feature sense. The theoretical mathematical background was proposed and it can be easily extended to other type of signals as long as they show non-linearities when raised to some power M.

Further work should be carried out regarding the use of other non-linear transformations that may be better adapted to the set of constellations we want to classify. Also, the study of advanced MAMC methods based on AMPT should be regarded, especially in the situation where the physical channel is not a simple impaired AWGN channel. This scenario would be relevant for cognitive satellite terrestrial radio (CSTR), land mobile SatComs or for terrestrial cellular networks.

Appendix A
Justification of Section V.

Denote $x_u(k) = s_u(k) \cdot h_u(t - k \cdot T)$ for better reading. We first apply the multinomial theorem to expand the power of the (infinite) sum as an infinite sum of infinite products.

$$y_u^M(t) = \sum_{\left(\sum_{j\in\mathbb{Z}} i_j\right)=M} \frac{M!}{\prod_{j\in\mathbb{Z}}(i_j!)} \prod_{j\in\mathbb{Z}} x_u^{i_j}(j) \tag{50}$$

In the sum, only $\tilde{M}$ terms i_j may be non-zero at the same time since the i_j are all positive integers. Then, we denote:

- $\tilde{M}$ the cardinality of the non-zero terms ($0 < \tilde{M} \leq M$)
- $\{k_j\}_{j\in\{1,\cdots,\tilde{M}\}}$ the $\tilde{M}$ indexes j such that i_j are non-zero

Thus, we can rewrite (50) as:

$$y_u^M(t) = \sum_{\substack{k_1<\cdots<k_{\tilde{M}} \\ 0<\tilde{M}\leq M}} \sum_{\substack{\left(\sum_{j=1}^{\tilde{M}} i_{k_j}\right)=M \\ i_{k_j}\neq 0}} \frac{M!}{\prod_{j=1}^{\tilde{M}}(i_{k_j}!)} \prod_{j=1}^{\tilde{M}} x_u^{i_{k_j}}(k_j) \tag{51}$$

It is then possible to invert the sums by re-indexing terms i independently from the k_j. This operation leads to:

$$y_u^M(t) = \sum_{\substack{0<\tilde{M}\leq M \\ \left(\sum_{j=1}^{\tilde{M}} i_j\right)=M \\ i_j\neq 0}} \sum_{k_1<\cdots<k_{\tilde{M}}} \frac{M!}{\prod_{j=1}^{\tilde{M}}(i_j!)} \prod_{j=1}^{\tilde{M}} x_u^{i_j}(k_j) \tag{52}$$

Following the fact that $0! = 1$ and $x_u^0 = 1$, the set in the first sum can be performed in the condensed generic set $\mathcal{I}_M$ (11) and the second sum in generic set $\mathcal{K}_M^{\mathbf{i}}$ (14). $\tilde{M}$ can simply be replaced by M in both the right-hand side products.

Then, we take the expectation of $y_{u,\mathbf{i}}(t)$. Remarking that that $h_u^{i_j}(t - k_j T)$ is deterministic for a given $\{\mathbf{i}, \mathbf{k}, t\}$ yields:

$$\mathbb{E}\left[y_{u,\mathbf{i}}(t)\right] = \sum_{\mathbf{k}\in\mathcal{K}_M^{\mathbf{i}}} \mathbb{E}\left[\prod_{j=1}^{M} s_u^{i_j}(k_j)\right] \prod_{j=1}^{M} h_u^{i_j}(t - k_j \cdot T) \tag{53}$$

The Poisson Summation Formula (PSF) is given by

$$\sum_{k\in\mathbb{Z}} g(t - kT) = \frac{1}{T} \sum_{m\in\frac{1}{T}\mathbb{Z}} e^{i\cdot mt} \cdot \mathcal{G}(m) \tag{54}$$

where $\mathcal{G}(f)$ stands for the Fourier Transform of $g(t)$.

Remarking that (53) can be written as

$$\mathbb{E}\left[y_{u,\mathbf{i}}(t)\right] = \sum_{k\in\mathbb{Z}} g(t - kT) \tag{55}$$

where

$$g(t - kT) = \sum_{\mathbf{k}\in\mathcal{K}_M^{0\mathbf{i}}} \mathbb{E}\left[\prod_{j=1}^{M} s_u^{i_j}(k_j)\right] \prod_{j=1}^{M} h_u^{i_j}(t - kT - k_j T) \tag{56}$$

makes it possible to apply the PSF to $g(t - kT)$, yields (15).

Appendix B
Justification of Section VI.

Lets unfold the expression of $\lambda_{\mathbf{m}}$ from (7) and (25):

$$\lambda_{\mathbf{m}} = \left| \mathcal{F}\left(\sum_{\mathbf{m}'\in\mathcal{M}_U^M} \binom{M}{\mathbf{m}'} \prod_{u=1}^{U} y_u^{m'_u}(t) \right)(f_{\mathbf{m}}) \right|^{\frac{2}{M}} \tag{57}$$

Denoting by $\left(\circledast_{u=1}^{U} f_{ru}\right) = f_{r1} * \cdots * f_{rU}$ – where $*$ stands for the classical convolution – and considering the properties of the Fourier Transform, (57) may be written as:

$$\lambda_{\mathbf{m}} = \left| \left(\sum_{\mathbf{m}'\in\mathcal{M}_U^M} \binom{M}{\mathbf{m}'} \overset{U}{\underset{u=1}{\circledast}} \mathcal{F}\left(y_u^{m'_u}(t)\right) \right)(f_{\mathbf{m}}) \right|^{\frac{2}{M}} \tag{58}$$

At frequency $f_{\mathbf{m}}$, the terms in the sum in (58) are all null if $\mathbf{m}' \neq \mathbf{m}$ and if the frequencies $f_{\mathbf{m}'}$ for $\mathbf{m}' \in \mathcal{M}_U^M$ are all different. Moreover, $\mathcal{F}\left(y_u^{m_u}(t)\right)(f)$ is zero if $f \neq f_{m_u}$. Then, the convolution is a simple product at frequency $f_{\mathbf{m}}$. Yields:

$$\lambda_{\mathbf{m}} = \left| \binom{M}{\mathbf{m}} \prod_{u=1}^{U} \mathcal{F}\left(y_u^{m_u}(t)\right)(f_{\mathbf{m}}) \right|^{\frac{2}{M}} \tag{59}$$

Then, (34) is simply obtained by distributing the absolute value in the product and by remarking that $\left|\mathcal{F}\left(y_u^{m_u}(t)\right)(f_{\mathbf{m}})\right| = \left(a_u^2 \cdot \lambda_{u,m_u}\right)^{\frac{m_u}{2}}$.

APPENDIX C
JUSTIFICATION OF SECTION VII.

The Probability Density Functions (PDF) of the PSD of y^M under H_0 and H_1 were developed in the literature related to spectral analysis [28]. First, (40) can be obtained from (39) with a simple variable change. Then, (41) is derived as:

$$\lambda_{\mathbf{m}}^{ref} = \int_0^{\infty} p\left[M\mathrm{PT}_y(f_{\mathbf{m}}) = x\right] x \; dx \tag{60}$$

Replacing I_0 by its expression and inverting both sum and integral operators yields:

$$\lambda_{\mathbf{m}}^{ref} = \sum_{k=0}^{\infty} \frac{M\lambda_{\mathbf{m}}^{kM}}{(k!)^2 \eta_M^{2k+1}} \int_0^{\infty} x^{(k+1)M} \cdot e^{-\frac{x^M+\lambda_{\mathbf{m}}^M}{\eta_M}} \; dx \tag{61}$$

Replacing the integral by its expression may give:

$$\lambda_{\mathbf{m}}^{ref} = \sqrt[M]{\eta_M} e^{-\frac{\lambda_{\mathbf{m}}^M}{\eta_M}} \sum_{k=0}^{\infty} \frac{1}{(k!)^2} \left(\frac{\lambda_{\mathbf{m}}^M}{\eta_M}\right)^k \Gamma\left(1+k+\frac{1}{M}\right) \tag{62}$$

Denoting by $.^{(k)}$ the rising factorial and noting that $\Gamma\left(1+k+\frac{1}{M}\right) = \left(1+\frac{1}{M}\right)^{(k)} \cdot \Gamma\left(1+\frac{1}{M}\right)$ and that $k! = 1^{(k)}$, we finally get expression (41).

REFERENCES

[1] O. Vidal, G. Verelst, J. Lacan, E. Alberty, J. Radzik, and M. Bousquet, "Next generation High Throughput Satellite system," *IEEE First AESS European Conference on Satellite Telecommunications (ESTEL)*, 2012.

[2] R. Alegre-Godoy, N. Alagha, and M. A. Vazquez-Castro, "Offered Capacity Optimization mechanisms for Multi-beam Satellite Systems," *IEEE International Conference on Communications (ICC)*, 2012.

[3] J. Palicot (Supervised by), "Radio Engineering: from Software Radio to Cognitive Radio," *Wiley*, 2011.

[4] M. Hoyhtya et al., "Application of Cognitive Radio techniques to Satellite Communication," *IEEE International Symposium on Dynamic Spectrum Access Networks (DYSPAN)*, 2012.

[5] S. K. Sharma, S. Chatzinotas, and B. Ottersten, "Cognitive Beamhopping for Spectral Coexistence of Multibeam Satellites," *Future Network and Mobile Summit*, 2013.

[6] D. Christopoulos, S. Chatzinotas, and B. Ottersten, "User Scheduling for Coordinated Dual-Satellite Systems with Linear Precoding," *IEEE International Conference on Communications (ICC)*, 2013.

[7] A. Soysal, S. Ulukus, and C. Clancy, "Channel Estimation and Adaptive M-QAM in Cognitive Radio Links," *IEEE International Conference on Communications (ICC)*, pp. 4043–4047, 2008.

[8] J. Palicot and C. Roland, "A New Concept for Wireless Reconfigurable Receivers," *IEEE Communications Magazine*, vol. 41, no. 7, 2003.

[9] M. Zaerin and B. Seyfe, "Multiuser Modulation Classification based on Cumulants in AWGN channel," *IET Signal Processing*, 2012.

[10] C. M. Spooner, "Classification of Co-channel Communication Signals using Cyclic Cumulants," *Proceedings of ASILOMAR-29*, 1996.

[11] V. Gouldieff, J. Palicot, and S. Daumont, "Blind Digital Modulation Classification based on Mth-Power Nonlinear Transformation," *IEEE Global Conference on Signal and Information Processing*, 2016.

[12] V. Weerackody, "Sensitivity of Satellite Interference to Locations of Small-Aperture Terminals," *IEEE Transactions on Aerospace and Electronic Systems*, 2016.

[13] S. Chatzinotas, G. Zheng, and B. Ottersten, "Joint Precoding with Flexible Power Constraints in Multibeam Satellite Systems," *IEEE Globecom*, 2011.

[14] K. Liolis et al., "Cognitive Radio Scenarios for Satellite Communications: the CoRaSat Approach," *Future Network and MobileSummit Conference*, 2013.

[15] Comtech, "CDM-625 Advanced Satellite Modem," *User Manual*, 2013.

[16] J. E. Mazo, "Jitter Comparison of Tones Generated by Squaring and by Fourth-Power Circuits," *Bell System Technical Journal*, 1978.

[17] O. A. Dobre, A. Abdi, Y. Bar-Ness, and W. Su, "Survey of Automatic Modulation Classification Techniques: Classical Approaches and New Trends," *IET Communications*, vol. 1, no. 2, pp. 137–156, 2007.

[18] A. Hazza, M. Shoaib, S. A. Alshebeili, and A. Fahad, "An Overview of Feature-based Methods for Digital Modulation Classification," *ICCSPA*, vol. 1, no. 08, pp. 1–6, 2013.

[19] A. Swami and B. M. Sadler, "Hierarchical Digital Modulation Classification using Cumulants," *IEEE Transactions on Communications*, 2000.

[20] O. A. Dobre, A. Abdi, Y. Bar-Ness, and W. Su, "Cyclostationarity-Based Modulation Classification of Linear Digital Modulations in Flat Fading Channels," *Wireless Personal Communications*, 2010.

[21] W. A. Gardner and C. M. Spooner, "The Cumulant Theory of Cyclostationary Time-Series, Part I: Foundation," *IEEE Transactions on Signal Processing*, 1994.

[22] C. M. Spooner and W. A. Gardner, "The Cumulant Theory of Cyclostationary Time-Series, Part II: Development and Applications," *IEEE Transactions on Signal Processing*, 1994.

[23] O. A. Dobre, M. Oner, S. Rajan, and R. Inkol, "Cyclostationarity-Based Robust Algorithms for QAM Signal Identification," *IEEE Communications Letters*, no. 1, 2012.

[24] J. Reichert, "Automatic Classification of Communication Signals using Higher Order Statistics," *IEEE International Conference on Acoustics, Speech, and Signal Processing*, vol. 5, no. 4, pp. 221–224, 1992.

[25] C. W. Lim and M. B. Wakin, "Automatic Modulation Recognition for Spectrum Sensing using Nonuniform Compressive Samples," *IEEE International Conference on Communications (ICC)*, 2012.

[26] H. J. Ryser, "Combinatorial Mathematics," *Mathematical Association of America (Book)*, 1963.

[27] C. Chatfield, "The Analysis of Time Series: An Introduction," *Book, 4th Ed. Chapman and Hall*, 1989.

[28] G. Jenkins and D. Watts, "Spectral Analysis and Its Applications," 1968.

Vincent Gouldieff received the Engineer degree in Electrical and Computer science from Supelec, France, in September 2014. He received the Master of Science I-MARS (Micro-technologies, Architecture, Networks and Communication Systems) from the National Institute for Applied Sciences, Rennes. From October 2014, he is a Ph.D candidate at the SCEE (Signal, Communication and Embedded Electronics) research team, Rennes, France, in CIFRE partnership with Zodiac Data Systems, Caen, France. His main research topics are related to blind signal processing methods, especially applied for satellite communication systems.

Prof. Jacques Palicot received, in 1983, his Ph.D degree in Signal Processing from the University of Rennes. Since 1988, he has been involved in studies about equalization techniques applied to digital transmissions and analog TV systems. Since 1991 he has been involved mainly in studies concerning the digital communications area and automatic measurements techniques. He has taken an active part in various international bodies EBU, CCIR, URSI, and within RACE, ACTS and IST European projects. He has published various scientific articles notably on equalization techniques, echo cancellation, hierarchical modulations and Software Radio techniques. He is author or co-author of more than 300 publications with more than 50 in journals, two books and 22 patents. He is currently involved in adaptive Signal Processing, digital communications, Software Radio, Cognitive radio and Green Radio. From November 2001 to September 2003 he had a temporary position with INRIA/IRISA in Rennes. He serves as Associate Editor for EURASIP JASP since 2008. He also served as lead guest editor for several Special Issues on Software Radio, Cognitive Radio and Green Radio. He was Co General Chairman of ISCIT 2011, Co General Chairman of Next-GWiN 2014, Technical Program Chairman of CROWNCOM 2009, Technical Program Chairman of GREENCOM 2013 and Technical Program Chairman of CRN Symposium of ICC 2014. Since October 2003 he is with CentraleSuplec in Rennes where he leads the Signal Communications and Embedded Electronics (SCEE) research team.

Dr. Steredenn Daumont received the engineering degree in Electronics from ENSSAT, Lannion, France, in 2006. She received the Ph.D degree in signal processing and telecommunication from the University of Rennes 1, Institute of Electronics and Telecommunications of Rennes (IETR), SCEE Team, Supelec, in 2009. From 2006 to 2009, she worked on blind sources separation of MIMO signals and on PAPR, in the SCEE team. Since 2010, she has been working at Zodiac Data Systems. Her research interests are in signal processing for communications, blind sources separation and characterisation of satellite signals.